

# Production and Decay of the $\Lambda_c$ Charmed Baryon from Fermilab E791.

B. Meadows <sup>1</sup>

*University of Cincinnati, Cincinnati, OH, 45221, USA*

**Abstract.** Results are presented for the 500 GeV/c pion production asymmetry and polarization of the  $\Lambda_c$  ( $\bar{\Lambda}_c$ ) charmed baryon from Fermilab experiment E791. An analysis of the decay to the  $p\bar{K}\pi$  final state is described. Resonant sub-channel fractions **and phases** are given and possible resonant effects in the low mass  $p\bar{K}$  system discussed. Significant decay to  $\Lambda_c \rightarrow \Delta^{++} K^-$  establishes for the first time the importance of a  $W$  exchange mechanism in charmed baryon decay.

Measurements of asymmetry  $A_{\mathcal{P}} = (d\sigma_{\mathcal{P}} - d\sigma_{\bar{\mathcal{P}}}) / (d\sigma_{\mathcal{P}} + d\sigma_{\bar{\mathcal{P}}})$  in the yield of particle  $\mathcal{P}$  and anti particle  $\bar{\mathcal{P}}$  can provide information on the production mechanisms involved. Dependences of  $A$  on  $x_F$  and  $p_T^2$  can distinguish different production models. Several experiments [1, and refs 1-9 therein] have shown that production of charmed mesons is characterized by leading particle effects and that asymmetries can be large. Leading particle behaviour has also been observed in production of strange hyperons in E791 [2] - even in a very central region.

Branching fractions for baryon decays provide information on the relative importance of lowest order decay mechanisms -  $W$  exchange or spectator processes. In  $\Lambda_c \rightarrow pK\pi$  decay, <sup>2</sup>  $W$  exchange can contribute to  $pK^{*0}$ ,  $\Lambda^*\pi$ ,  $\Sigma^*\pi$  or  $pK\pi$  channels, but for the  $\Delta^{++}K^-$  mode it is the *only* low order process possible. Evidence for this decay requires a large sample of  $pK\pi$  decays and proper analysis of interference effects in the system.

Reported here are the first published [3] measurements of both  $x_F$  and  $p_T^2$  dependence of  $A$  for charmed baryon production. We also present [4] the first full analysis of charmed baryon decay, measuring  $\Lambda_c$  branching fractions, relative phases and polarization.

This study is based on a sample of  $2 \times 10^{10}$  events produced from the interaction of 500 GeV/c  $\pi^-$  incident on thin foils, one  $Pt$  and four  $C.Pt$  target data (unequal numbers of  $n$  and  $p$ ) were not used in the asymmetry study. The detector and data reconstruction are described in [5]. Cuts on geometric and kinematic quantities were made to identify  $\Lambda_c \rightarrow pK^-\pi^+$  decays. The decay vertex had to be well separated ( $> 5\sigma$ ) from both production vertex and nearest target material. The yield, shown in Fig. 1(a)-(d), was  $1,025 \pm 45$   $\Lambda_c \rightarrow pK^-\pi^+$  and  $794 \pm 42$   $\bar{\Lambda}_c \rightarrow \bar{p}K^+\pi^-$ . Events were divided into 5 regions of  $x_F$  and 5 of  $p_T^2$  in the overall ranges:  $-0.1 < x_F < 0.6$  and  $p_T^2 \leq 8$  (GeV/c)<sup>2</sup> chosen to have clear  $\Lambda_c$  signals in each. Fits similar to those shown in the figure were made to each sample to determine the number  $N(\Lambda_c)$  and  $\bar{N}(\bar{\Lambda}_c)$  of signal events in each range.

---

<sup>1</sup> Representing the E791 Collaboration

<sup>2</sup> Note that charged conjugate states are implied unless stated otherwise.

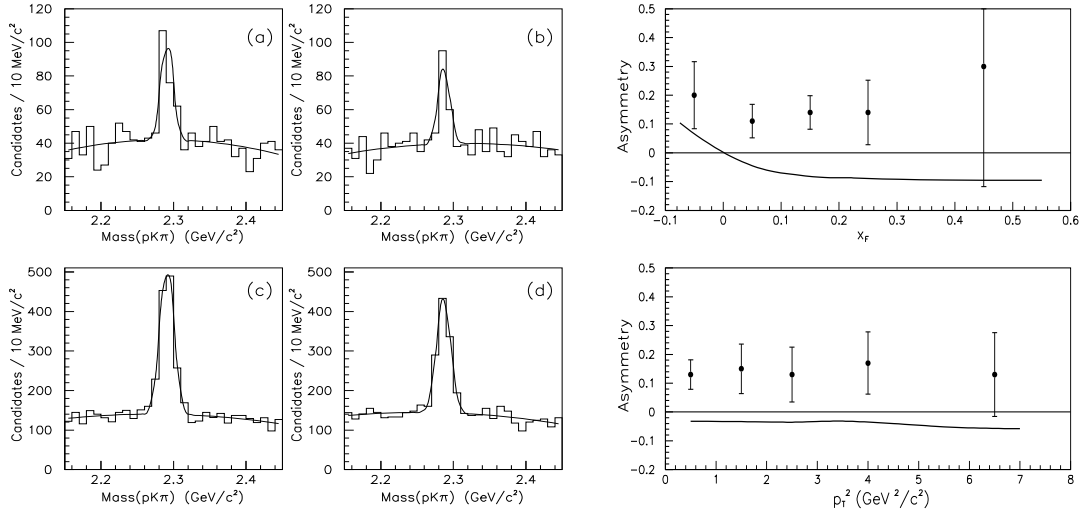


**FIGURE 1.**  $\Lambda_c(\bar{\Lambda}_c)$  samples: (a)  $\Lambda_c$  ( $x_F < 0$ ); (b)  $\bar{\Lambda}_c$  ( $x_F < 0$ ); (c)  $\Lambda_c$  ( $x_F > 0$ ); (d)  $\bar{\Lambda}_c$  ( $x_F > 0$ ). Fits shown in (a)-(d) are Gaussian peaks on 2nd order polynomial backgrounds. Asymmetries: (e) vs  $x_F$  (f) vs  $p_T^2$ . The solid curves in (e) and (f) are the prediction of Pythia/Jetset.

## $\Lambda_c/\bar{\Lambda}_c$ ASYMMETRIES

Efficiencies  $\epsilon$  ( $\bar{\epsilon}$ ) for  $\Lambda_c(\bar{\Lambda}_c)$  were not quite equal due to the asymmetric effect of the intense  $\pi^-$  beam on the drift chambers. This effect was greatest at large  $x_F$  and low  $p_T^2$ . It was necessary therefore to estimate the ratio  $r = \epsilon/\bar{\epsilon}$  in each of the 5  $x_F$  and 5  $p_T^2$  ranges using Monte Carlo samples of  $\Lambda_c$  &  $\bar{\Lambda}_c$  generated with Pythia/Jetset, projected through a simulated E791 detector and subjected to the same reconstruction code and selection criteria as the data. Corrected asymmetries  $A = (N - \bar{N}/r)/(N + \bar{N}/r)$  were then obtained in each range.

The main sources of systematic uncertainty (parametrization of signal and background shapes and precision of  $r$ ) amounted to less than 50% of the statistical uncertainty in all instances. The results are shown in Figure 1(e) and (f) and compared with earlier  $\pi^- N$  studies in Table 1.

**TABLE 1.** Comparison with asymmetries (%) from earlier  $\pi^- N$  experiments.

$x_F$ region	E791	ACCMOR [6]	SELEX [7]
$x_F < 0$	$20 \pm 10 \pm 6$	—	—
$x_F > 0$	$12.3 \pm 3.7 \pm 1.6$	$0.5 \pm 7.9$	$25 \pm 15$

The asymmetry is positive and flat throughout the range. This might result from the additional energy required to produce additional baryons when a  $\Lambda_c$  is produced, favouring  $\Lambda_c$  production in general. The solid curve in Figure 1 is the prediction of Pythia/Jetset and clearly does not describe the data well. Two component intrinsic charm/coalescence models [8], [9] predict a rising asymmetry beginning at the low end or possibly below the range of this data. Leading particle effects would also result in a

rising asymmetry in the entire  $x_F < 0$  region. The data do not rule that possibility out.

## ANALYSIS OF THE DECAY $\Lambda_c \rightarrow PK^-\pi^+$

A cleaner sample was required for this analysis. The length cut was increased to  $8\sigma$  and a neural net criterion was used to optimize the significance  $S/\sqrt{S+B}$  of the signal ( $S = 886 \pm 43$ ) over background ( $B \sim 300$ ) in the fit region.

These decays were defined by five independent variables, e.g. two Dalitz plot coordinates and orientation of the decay plane relative to production plane ( $z$  axis). The  $\Lambda_c$  could have polarization  $P_{\Lambda_c}\hat{z}$ .

Each isobar decay channel  $\Lambda_c \rightarrow R(\rightarrow ab)c$  was assigned an amplitude labeled by the  $z$  component of  $\Lambda_c$  spin,  $m$ , and proton helicity ( $\pm\frac{1}{2}$ ) in the  $\Lambda_c$  rest frame

$\mathcal{A}_{m,\pm\frac{1}{2}}^R = B^R(M_{ab})(a_{\pm}e^{i\alpha_{\pm}}|m,\pm\frac{1}{2},\lambda_{\alpha_{\pm}}> + b_{\pm}e^{i\beta_{\pm}}|m,\pm\frac{1}{2},\lambda_{\beta_{\pm}}>)$  where  $\lambda_{\alpha_{\pm}}$  &  $\lambda_{\beta_{\pm}}$  are the two possible helicities for  $R$  with unknown coefficients  $a_{\pm}e^{i\alpha_{\pm}}$  &  $b_{\pm}e^{i\beta_{\pm}}$ . The  $B^R(M_{ab})$  were Breit Wigner functions. For non-resonant  $NR$  decay to  $pK\pi$  a similar amplitude with  $B = 1$  was used. An unbinned, maximum likelihood fit was used to determine  $a_{\pm}, \alpha_{\pm}, b_{\pm}, \beta_{\pm}$  and three values for  $P_{\Lambda_c}$  (one in each of three  $x_F$  ranges). The signal probability density function was

$$\begin{aligned} \mathcal{P}_s = & \frac{1}{2} \times \epsilon \times [(1 + P_{\Lambda_c}) \left( \left| \sum_R \mathcal{A}_{\frac{1}{2}, \frac{1}{2}}^R \right|^2 + \left| \sum_R \mathcal{A}_{\frac{1}{2}, -\frac{1}{2}}^R \right|^2 \right) \\ & + (1 - P_{\Lambda_c}) \left( \left| \sum_R \mathcal{A}_{-\frac{1}{2}, \frac{1}{2}}^R \right|^2 + \left| \sum_R \mathcal{A}_{-\frac{1}{2}, -\frac{1}{2}}^R \right|^2 \right)] \end{aligned}$$

Five dimensional efficiency ( $\epsilon$ ) and background density were estimated empirically from a MC sample and  $M_{pK\pi}$  sidebands. Modes included were  $p\bar{K}^{*0}(890)$ ,  $\Delta^{++}(1232)K^-$ ,  $\Lambda(1520)\pi^+$  and  $NR$ .

The fit shown in Figure 2 is seen to be good except for the low mass  $K^-p$  region where an unmodelled enhancement is seen. Many  $Y^*$  exist which could possibly account for this. Each  $Y^*\pi$  channel added to our fit requires  $\geq 4$  more parameters making it difficult, with our limited sample, to include more than one  $Y^*$ . Adding  $\Lambda(1600)\pi$ ,  $\Sigma(1600)\pi$  or the tail of the  $\Sigma(1405)\pi$  alone made no significant improvement.

Isobar fractions  $f_R$  were computed by integrating over the five dimensions of the fit  $\vec{x}$ :

$$f_R = \int \sum_{m,\pm\frac{1}{2}} \left| \mathcal{A}_{m,\pm\frac{1}{2}}^R \right|^2 d\vec{x} / \int \sum_{m,\pm\frac{1}{2}} \left| \sum_R \mathcal{A}_{m,\pm\frac{1}{2}}^R \right|^2 d\vec{x}$$

Branching ratios with respect to  $pK^-\pi^+$  are compared with earlier results in Table 2.

Good agreement is seen, but the significance of signals from NA32, where only mass projections were fit is overestimated. NA32 errors are comparable to E791, but E791's sample is much larger. This is because correlations among channels and relative phases were neglected in the NA32 analysis.

The  $\Delta^{++}K^-$  mode is comparable to  $p\bar{K}^{*0}$  and clearly significant.

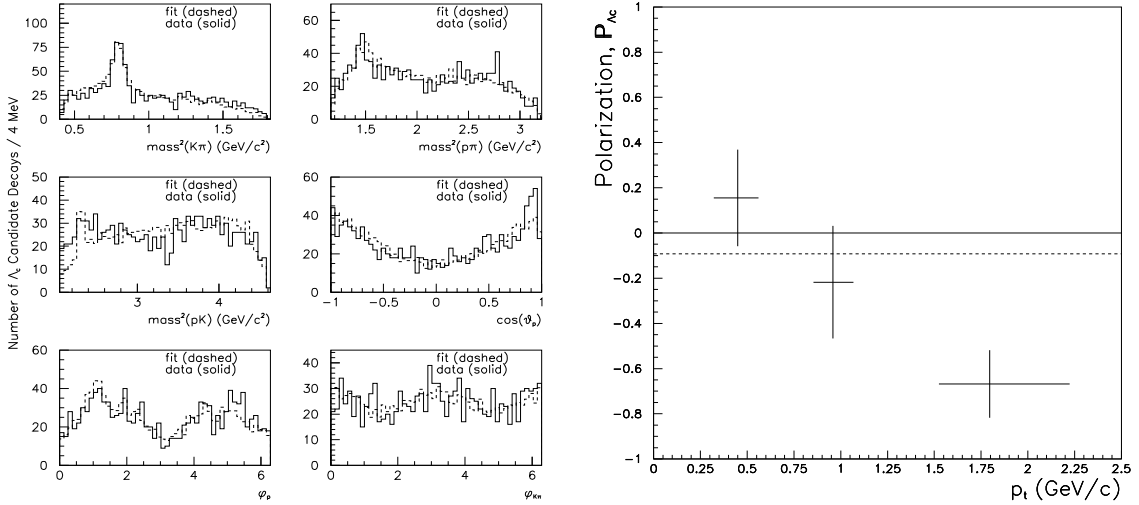


**FIGURE 2.** **Left:** Projections of fit (dashed lines) onto three mass pair and three angular variables (solid lines). Data lie in the range  $2265 < M(pK\pi) < 2315$  MeV/c $^2$ . **Right:**  $\Lambda_c/\overline{\Lambda}_c$  Polarization from fit.

**TABLE 2.** First three columns are branching fractions relative to total  $pK\pi$  mode (%) corrected for unseen decays). The last four columns are resonant phases, described in the text, measured only by E791.

Mode	E791	NA32	ISR	E791 relative phases (degrees)			
				[10]	[11]	$\alpha_+$	$\beta_+$
$pK^{*0}(890)$	$29 \pm 4 \pm 3$	$35^{+6}_{-7} \pm 3$	$42 \pm 24$	$58 \pm 28$	$135 \pm 38$	$198 \pm 24$	$303 \pm 32$
$\Delta^{++}(1232)K^-$	$18 \pm 3 \pm 3$	$12^{+4}_{-5} \pm 5$	$40 \pm 17$	$285 \pm 23$	$280 \pm 23$	$= \alpha_+$	$= \beta_+$
$\Lambda(1520)\pi^+$	$15 \pm 4 \pm 2$	$9^{+4}_{-3} \pm 2$	—	$340 \pm 30$	$-3 \pm 32$	$= \alpha_+$	$= \beta_+$
NR	$55 \pm 6 \pm 4$	$56^{+7}_{-9} \pm 5$	—	$199 \pm 31$	0 (fixed)	$43 \pm 41$	$65 \pm 21$

## SUMMARY

$\Lambda_c$  production asymmetry in the range  $-0.1 < x_F < 0.6$  and  $p_T^2 < 8$  (GeV/c) $^2$  is constant at  $\sim +0.15$  favouring  $\Lambda_c$  over  $\overline{\Lambda}_c$ . Models requiring a rising asymmetry toward negative  $x_F$  are not ruled out however. An amplitude analysis of the  $\Lambda_c$  decay shows the  $\Lambda_c \rightarrow \Delta^{++}K^-$  mode to be large indicating that the  $W$  exchange amplitude is important.

## REFERENCES

1. E791 Collaboration (E.M. Aitala *et al.*), *Phys. Lett.*, **B411**, 230 (1997).
2. E791 Collaboration (E.M. Aitala *et al.*), *Phys. Lett.*, **B496**, 9 (2000).
3. E791 Collaboration (E.M. Aitala *et al.*), *Phys. Lett.*, **B495**, 42 (2000).
4. E791 Collaboration (E.M. Aitala *et al.*), *Phys. Lett.*, **B471**, 449 (2000).
5. E. Aitala *et al.*, *EPJdirect* **C4**, 1 (1999); P. Karchin *et al.*, *IEEE NS* **32**, 612 (1985); D. Bartlett *et al.*, *NIM* **A260**, 55 (1987); V. Bharadwaj *et al.*, *NIM* **155**, 411 (1978); **A228**, 283 (1985); D. Summers, *NIM* **A228**, 290 (1985); J. Appel *et al.*, *NIM* **A243**, 361 (1986); S. Amato *et al.*, *NIM* **A324**, 535 (1993); F. Rinaldo *et al.*, *Comput. Phys.* **7**, 184 (1993); S. Bracker *et al.*, *IEEE NS* **43**, 2457 (1996).
6. ACCMOR Collaboration (S. Barlag *et al.*), *Phys. Lett.*, **B247**, 113 (1990).
7. M. Iori *et al.*, EPS-HEP99 conference, Tampere, Finland (15–21 July 1999), hep-ex/9910039.
8. R. Vogt and S. J. Brodsky, *Nucl. Phys.*, **B478**, 311 (1996).
9. G. Herrera and J. Magnin, *Eur. Phys. J.*, **C2**, 477 (1998).
10. ACCMOR Collaboration (A. Bozek *et al.*), *Phys. Lett.*, **B312**, 247 (1993).
11. Split Field Magnet Collaboration (M. Basile *et al.*), *Nuovo Cimento*, **62A**, 14 (1981).